This article has been published in: Journal of Dentistry 2018. pii: S0300-5712(18)30537-2.

Acknowledgements

This work was supported by the Ministry of Economy and Competitiveness (MINECO) and European Regional Development Fund (FEDER). Project MAT2017-85999-P MINECO/AEI/FEDER/UE.

Title: Silver improves collagen structure and stability at demineralized dentin: a dynamic-mechanical and Raman analysis.

Short title: Ag improved collagen at demineralized dentin.

Authors: Raquel Osorio[a], Estrella Osorio[a], Fátima S. Aguilera[a], Antonio Luis Medina-Castillo[b], Manuel Toledano[a*], Manuel Toledano-Osorio[a].

Institution: [a]University of Granada, Faculty of Dentistry, Dental Materials Section.

Colegio Máximo de Cartuja s/n

18071 – Granada - Spain.

[b]University of Granada, NanoMyP. Spin-Off Enterprise.

Edificio BIC-Granada. Av. Innovación 1.

18016 - Armilla, Granada, Spain.

***Corresponding author:**

Prof. Manuel Toledano.

University of Granada, Faculty of Dentistry

Dental Materials Section

Colegio Máximo de Cartuja s/n

18071 – Granada - Spain.

Tel.: +34-958243789

Fax: +34-958240809

Email: toledano@ugr.es

Highlights

Ag-NPs improved both structure and stability of collagen at the demineralized dentin

Ag-NPs may be indicated in Dentistry to preserve demineralized organic matrix

Ag-NPs application may retard functional remineralization of dentin

Graphical abstract

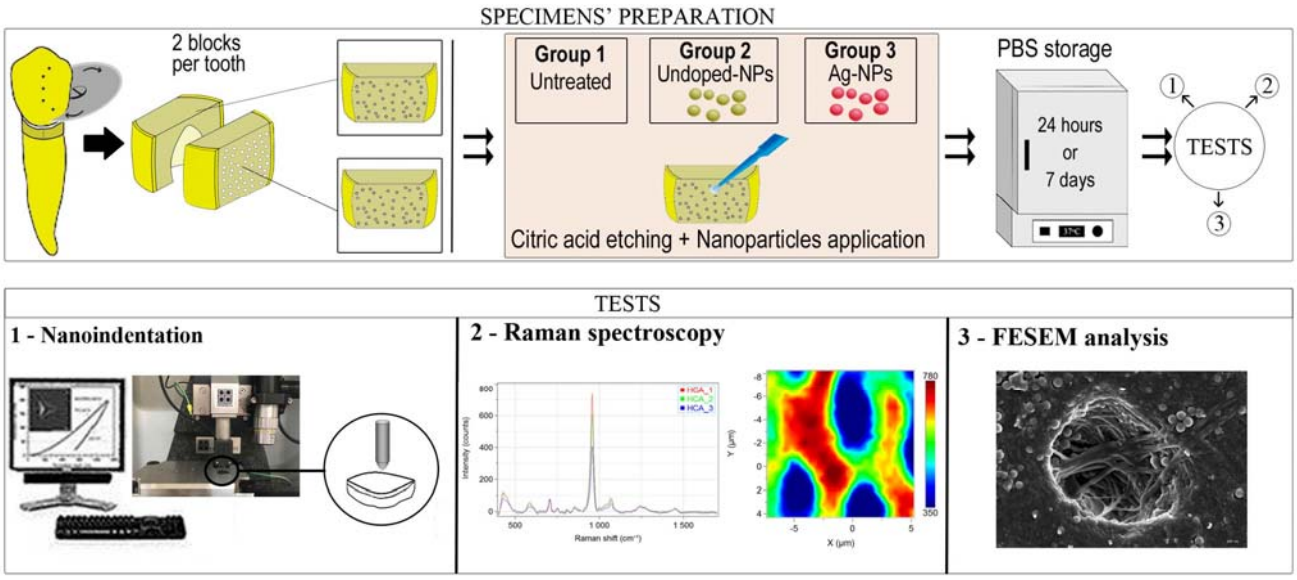

ABSTRACT

Objective: This study aimed to evaluate the effect of silver loaded nanoparticles (NPs) application on dentin remineralization.

Methods: Polymethylmetacrylate-based NPs and silver loaded NPs (Ag-NPs) were applied on demineralized dentin surfaces. Dentin was characterized morphologically by scanning electron microscopy, mechanically probed by a nanoindenter to test nanohardness and Young modulus, and chemically analyzed by Raman spectroscopy after 24 h and 7 d of storage. Untreated surfaces were used as control. Data were submitted to ANOVA and Student-Newman-Keuls multiple comparisons tests ($P<0.05$).

Results: After Raman analysis, dentin treated with Ag-NPs obtained the lowest mineralization and intensity of stoichiometric hydroxyapatite when compared with specimens treated with undoped-NPs. The lowest relative mineral concentration, expressed as the ratio phosphate or carbonate/phenyl group, and crystallinity was attained by dentin treated with with Ag-NPs, after 7 d. Ag-NPs application generated the highest values of collagen crosslinking (intensity at 1032 cm^{-1} band). The molecular conformation of the collagen's polypeptide chains, amide-I and CH_2 also attained the highest peaks in dentin treated with Ag-NPs. Staggered and demineralized collagen fibrils were observed covering the dentin surfaces treated with Ag-NPs, at both 24 h and 7 d. Samples treated with Ag-NPs attained the lowest values of nanohardness and Young's modulus at 7 d of storage.

Conclusions: Peritubular and intertubular dentin were remineralized when using undoped-NPs. After 7 d, collagen treated with NPs was remineralized but dentin treated with Ag-NPs attained an improved collagen matrix structure and stability but the lowest mineralization and crystallinity.

Clinical significance: Preservation of the demineralized organic matrix is fundamental in operative dentistry. Silver contributed to improve crosslinking, nature and secondary structure of demineralized dentin collagen, for further long-term intrafibrillar mineralization.

Key words: Collagen, erosion, demineralisation, dentine, microscopy, Raman.

1. Introduction

Acids demineralize dentin. The acid can arise from bacteria (causing dental caries), from acid etching during dental procedures, or even from food, beverages or gastric juice (causing dental erosion) [1]. Dentin-erosive demineralization results in the exposure of an outer layer of fully demineralized and sometimes denatured organic matrix [2]. The remineralization process of mineral depleted dentin is crucial when eroded dentin is going to become treated [1]. Some resins, varnishes and remineralizing agents [3] have been proposed to treat eroded or caries-affected dentin, but most of them do not promote functional remineralization, do not demonstrate enough compatibility [4], and their effects are often temporal [5].

The biological reconstruction of the demineralized substrate is one of the primary goals of conservative dentistry [6]. The essential elements for successful treatment of demineralized dentin are eliminating or reducing bacterial biofilm [7] and improving dentin remineralization [8]. Therefore, the development of novel antibacterial and remineralizing dental materials is needed to combat caries and protect tooth structures [9].

Silver nanoparticles, due to their antibacterial properties have been previously used in dentin adhesive formulations [10–12]. The use of polymeric nanoparticles (NPs), as calcium and phosphate sequestering materials, to facilitate dentin remineralization has been earlier stated [13,14]. The proposed polymeric nanoparticles (NPs) may be silver-loaded, as anionic carboxylate sequences on the NPs surfaces (COO^-) allow the complexation of cationic ions [13]. This feature results in a higher proportion of material exposed for the potential reaction, which needs a lower concentration of silver to reach the same effect of silver at the microscale [11]. Then, NPs may be excellent platforms for the efficient delivery of antibacterial and other bioactive agents [15].

Silver addition has demonstrated specific antibacterial activity at the resin-dentin interface [10–12], but studies on the effect of silver on dentin remineralization are also required. Ag-NPs regulate the deposition of collagen and inhibit uncontrolled growth of collagen, as well as they direct proper collagen matrix alignment and spatial arrangement [16]. To date, some research has focused on the effect of silver on bone remineralization [17,18]. Those assays performed on dentin [1,6,19] resulted controversial and they are difficult to interpret, as they use not only silver but other ions as fluoride, nitrate or calcium in combination. However, there are few studies of Zn or Ca-loaded NPs [13,15] application on dentin, but the effects of Ag-NPs on the static mechanical properties and physic-chemical characterization of treated dentin are unknown.

Although nano-mechanical tests and Raman analysis have been conducted on dentin in previous researches, none was performed after Ag-NPs application on dentin surfaces. The aim of this study was to investigate the effect of silver application on dentin remineralization. Mechanical, chemical and histo-morphological changes occurring after treating dentin surfaces with Ag-NPs were analyzed. The null hypothesis was that no changes in morphological, mechanical and chemical properties were produced at dentin surfaces after Ag-NPs application.

2. Materials and methods

2.1. Nanoparticles production

PolymP-*n* Active nanoparticles (NPs) (NanoMyP, Granada, Spain) were fabricated trough polymerization precipitation [20]. NPs are composed by 2-hydroxyethyl methacrylate (backbone monomer), ethylene glycol dimethacrylate (cross-linker) and methacrylic acid (functional monomer). For silver complexation on NPs, 30 mg of NPs were immersed at room temperature, during 3 days under continuous shaking in 15 ml aqueous solution of $AgNO_3$ (containing Ag at 40 ppm at pH 6.5), in order to reach the adsorption equilibrium of metal ions [13]. Two different NPs were tested: 1) NPs (NPs) and 2) silver doped NPs (Ag-NPs).

2.2. Specimens' preparation

Fifteen human third molars, extracted for surgical reasons, without caries lesions were obtained with informed consent from donors (20–40 year of age), under a protocol approved by the Institution Review Board (405/CEIH/2017). Two dentin blocks from the buccal surfaces of each root, just below the cement-dentinal junction were obtained by cutting with a diamond saw (Accutom-50 Struers, Copenhagen, Denmark) under copious water irrigation.

The surfaces were polished through SiC abrasive papers from 800 up to 4000 grit followed by final polishing steps. Dentin blocks were demineralized by 1% citric acid (pH 3.8) for 1 min, in order to expose type I collagen fibrils of dentin dissolving the calcium-phosphate mineral phases to form a porous collageneous surface layer [21]. A PBS suspension of NPs, Ag-NPs (10 mg/ml) or just a PBS solution were applied (30 s), in each of the three different experimental groups. For each tooth, one of the two treated dentin blocks specimens were stored in PBS at 37º C for 24 hours and the other for 7 days.

2.3. Nanoindentation

The nanoindentation process was performed using a HysitronTi 950 nanoindenter (Hysitron, Inc., Minneapolis, MN). The nanoindenter was a Berkovich (three-sided pyramidal) diamond indenter tip (tip radius ~20 nm). It was calibrated against a fused quartz sample using a quasistatic force setpoint of 5 μN. Ten indentations with a peak of load of 4000 μN and a time function of 10 s were performed on each dentin sample at peritubular (PD) and intertubular dentin (ID) at 24 h and 7 d of storage. The procedure was performed in a hydrated condition by the application of a layer of ethylene glycol over the specimen surface. From this test, nanohardness (H_i) and nanoindentation modulus (E_i) of the samples, were obtained. The rest of the procedures were as in Oliver and Pharr, 1992 [22] and Toledano et al., 2017 [23]. Data were analyzed by two-way ANOVA (independent factors were NPs application and storage time) and Student-Newman-Keuls multiple comparisons ($P < 0.05$). Comparisons between storage times within the same groups were performed with Student *t* test ($P < 0.01$).

2.4. Statistical Analysis

For data normality and homogeneity of variance assumptions Kolmogorov-Smirnov and Levene's tests were employed ($P>0.05$). Data were analyzed by two-way ANOVA including interactions. Independent factors were NPs application and storage time. Student-Newman-

Keuls was used for multiple comparisons ($P<0.05$). Comparisons between storage times within the same NPs application group were performed with Student *t* test ($P<0.01$).

2.5. Raman spectroscopy

The same dentin surfaces were, then, submitted to Raman analysis using a dispersive Raman spectrometer/microscope (Horiba Scientific Xplora, Villeneuve d´Ascq, France). Raman signal was acquired using a 600-lines/mm grafting centered between 400 and 1700 cm^{-1}. For each specimen two areas 12x12 µm of the dentin at different sites were mapped using 0.5 µm spacing at X and Y axis. This chemical mapping was submitted to K-means cluster (KMC) analysis using the multivariate analysis tool (ISys® Horiba), which includes statistical pattern to derive the independent clusters. The natural groups of components were calculated by the software and the Hierarchical Cluster Analysis (HCA).

As the cluster centroids are essentially means of the cluster score for the elements of cluster, the mineral and organic components of the dentin surfaces were examined for each cluster. A total of 625 points were performed per map. Clusters were created following Ward´s technique and the dendrogram was calculated applying three factor spectra or principal components, corresponding with three different components at the dentin surface (red, blue and green). At this point, the mineral (relative presence of minerals and crystallinity) and organic components (normalization, crosslinking, nature and secondary structure of collagen) of dentin was assessed as previously published [23,24].

2.6. Field Emission Scanning Electron Microscopy (FESEM)

After all the previous analyses, two specimens from each experimental group were fixed in a solution of 2.5% glutaraldehyde in 0.1 mol/L sodium cacodylate buffer for 24 h, rinsed three times in 0.1 mol/L sodium cacodylate buffer. Samples were placed in an apparatus for critical point drying (Leica EM CPD 300, Wien, Austria). They were then sputter-coated with carbon by means of a sputter-coating Nanotech Polaron-SEMPRE2 (Polaron Equipment Ltd., Watford, UK) and observed with a field emission scanning electron microscope (FESEM Gemini, Carl Zeiss, Oberkochen, Germany) at an accelerating voltage of 2.5 to 3 kV.

3. Results

The nanomechanical properties (*Hi* and *Ei)* of the dentin surfaces at ID and PD were influenced by NPs application ($P<0.05$) and by storage time ($P<0.05$). Interactions between factors were also significant ($P<0.05$). Mean and SD of *Hi* and *Ei* are represented in Table 1. Samples treated with Ag-NPs always attained the lowest *Ei* and *Hi* at PD and at ID (Table 1). At these experimental groups (Ag-NPs), no differences were encountered between the attained values (*Ei* and *Hi*) at 24 h or 7 d. Undoped NPs achieved the highest *Ei* and *Hi* values at ID after 7 d (Table 1).

Results from Raman analysis are presented in Table 2 and Figures 1 and 2. After 7 d, dentin treated with Ag-NPs attained lower degree of mineralization than dentin treated with undoped NPs, related to the phosphate (960 cm^{-1}) (Fig. 1C, Table 2) and carbonate (1070 cm^{-1}) bands (Table 2). Samples treated with Ag-NPs did also achieve the lowest values of mineralization concerning both relative mineral concentrations of phosphate (RMC_p) (Fig 1I) and carbonate (RMC_c) (Table 2) when compared with NPs treated and untreated dentin

(Table 2, Fig. 1G). Dentin treated with Ag-NPs obtained the highest full width at half maximum (FWHM) of the phosphate (PO_4^{3-}) band at 961 cm^{-1} (19.89) after 7 d of storage, showing the poorest crystallinity among groups (Fig. 2C) (Table 2). This complied with a lower height peak of both, the marker for calcification at 954 cm^{-1} (~520) and the stoichiometric hydroxyapatite (HAp) band v_1 at 963 cm^{-1} (~524), if compared to dentin treated with undoped-NPs after 7 d of storage (Table 2). After 7 d of storage, Ag-NPs application generated higher values of collagen crosslinking at the spectral bands of 1032 cm^{-1}. The molecular conformation of the collagen's polypeptide chains, amide-I (1655-1667 cm^{-1}) and CH_2 (1450 cm^{-1}) also attained the highest peaks at dentin treated with Ag-NPs, at 7 d time point (Table 2).

No mineral precipitation was observed at the FESEM images on the untreatred dentin specimens (Fig. 3A), but it was on dentin treated with undoped-NPs. The precipitated crystals appeared covering the intertubular and peritubular dentin (Fig. 3B). Dentin remineralization was neither observed at surfaces treated with Ag-NPs, where the tubule entrances appeared open (Figs. 3C, 3D). The prototypical D-periodicity banding of demineralized collagen fibrils were visible in dentin treated with Ag-NPs, stored for 24 h (Fig. 3C) or for 7 d (Fig. 3D).

4. Discussion

Ag-NPs may impair or retard functional remineralization of dentin as proved by testing nano-mechanical properties and chemical analysis of the relative mineral concentration. The general lower nano-mechanical properties at the dentin surface when Ag-NPs were applied and assessed at any time, in comparison with the rest of the groups (Table 1), is correlated with a lack of remineralizing effect [23]. This was linked to poor mineral precipitation (Ca and P) at the demineralized organic matrix [25] and to scarce functional remineralization [26,27]. Thus, silver seems to inhibit functional mineralization and mineral formations onto the demineralized dentin surfaces, allowing the exposure of the demineralized collagen (Fig. 3D·II).

After Raman analysis, these outcomes were corroborated. Thus, the corresponding HCA images (clusters) and results (centroids) obtained at the dentin surface treated with Ag-NPs (Fig. 2C), showed a generalized lower presence of phosphate in two of the three distinguishable centroids (HCA_2 and HCA_3) (green and blue areas and % variances) when compared to dentin treated with undoped-NPs (Fig. 2B). Higher mineral/matrix ratios (Table 2) (Fig. 1G) may be caused by the increase in phosphate or carbonate content or by a decrease in content of the organic matrix, as it occurred in the present study, at the untreated group (Fig. 1D). A higher FWHM (full-width-half-maximum) in Ag-NPs group (Table 2) means lower crystallographic maturity and crystallinity in minerals [28]. This low crystallinity usually became associated to, *i)* the minor phosphate v_1 vibration, at 963 cm^{-1} height [29] (Table 2) which corresponded to stoichiometric HAp, and deactivates dentin remodeling with decreased maturity [30,31]. The association between poor crystallinity and low mechanical properties, has been confirmed in the present research (Table 1). As mentioned above, no other specific studies testing dentin remineralization in the presence of silver have been previously performed, but Saito et al., 2003 [6] did show that silver impaired the mineral precipitation and/or HAp formation on the insoluble fraction of type I collagen. It was tested trough X-Ray diffraction, and mineral induction was decreased in a time and dose-dependent manner, forming a calcium-deficient HAp when silver was present [6]. However, if topical

application of silver is performed in combination with other ions (calcium or fluoride), mineral density of demineralized dentin lesions have been shown to increase [19].

Silver facilitates the proper collagen matrix alignment and spatial arrangement [16]. The raise of CH_2, Amide I and Ratio Amide I/A-III (Table 2) when Ag-NPs were applied indicated recovery [32], better organization, improved structural differences and collagen quality [33]. Then, Ag-NPs application would favor further mineralization, at the long term, because of the increase of collagen crosslinking [34].

The prototypical D-periodicity banding of collagen that was observed in dentin treated with Ag-NPs (Fig. 3D·II), therefore, may be attributable to the scarce affectation of collagen fibril by degradation, after demineralization [26]. Silver possesses a potent inhibitory effect on the activity of matrix-metalloproteinases (MMPs) [1]. One plausible explanation may be that Ag^{2+} occupies the site of Ca^{2+} within collagen fibrils, protecting collagen from MMPs trough a competitive inhibition, filling the MMPs' zinc binding sites at collagen. Silver ions have also been shown to interact with aminoacids in proteins, and specifically have high affinity to bond to carboxylate groups [35]. This hypothesis is in accordance with a previous study by Matthiessen et al.,1985 [36], in which silver methenamine was used to stain dentin and cementum collagen; it was found that only demineralized or hypomineralized collagen was stained. After staining, silver was encountered forming regularly arranged transverse bands (25 nm) with a periodicity of approximately 65 nm along the length of the fibril. Even more, those fibrils that were mineralized were unstained [36]. It may explain how the crosslinking (Table 1) and the D-periodicity banding were maintained in the absence of functional remineralization (as mechanical properties are not recovered at Ag-NPs treated dentin).

The proposed null hypothesis must be rejected. Present study is important as silver nanoparticles are currently being recommended not only for dentin applications [7,12] but also for bone regeneration [16,17]. However, there are some limitations to this experiment. As testing was performed after 7 d, it only reflected the short-term effects of used NPs. Thereby, it may be interesting as a practical approach to protect the demineralized collagen, by applying Ag-NPs together with other ions (fluoride, calcium…) to create an environment that favors the remineralization process. Further research, in this line, is being implemented.

5. Conclusions

Within the limits of this study, it can be concluded that silver is able to improve the chemical structure and stability of collagen at demineralized dentin. Besides it impairs or retards collagen fibril remineralization at demineralized dentin surfaces. An amorphous phase of formed HAp with decreased chemical stability is encountered in Ag-treated demineralized dentin surfaces. The HAp amorphization process became associated to low mechanical properties.

Declaration of interests

The authors declare that they have no conflict of interest.

References

[1] M.L. Mei, L. Ito, Y. Cao, Q.L. Li, E.C.M. Lo, C.H. Chu, Inhibitory effect of silver diamine fluoride on dentine demineralisation and collagen degradation, J. Dent. 41 (2013) 809–817. doi:10.1016/j.jdent.2013.06.009.

[2] J.H. Kinney, M. Balooch, D.L. Haupt, S.J. Marshall, G.W. Marshall, Mineral distribution and dimensional changes in human dentin during demineralization, J. Dent. Res. 74 (1995) 1179–1184. doi:10.1177/00220345950740050601.

[3] Z. Wang, T. Jiang, S. Sauro, D.H. Pashley, M. Toledano, R. Osorio, S. Liang, W. Xing, Y. Sa, Y. Wang, The dentine remineralization activity of a desensitizing bioactive glass-containing toothpaste: an in vitro study, Aust. Dent. J. 56 (2011) 372–381. doi:10.1111/j.1834-7819.2011.01361.x.

[4] L.N. Niu, W. Zhang, D.H. Pashley, L. Breschi, J. Mao, J.-H. Chen, F.R. Tay, Biomimetic remineralization of dentin, Dent. Mater. 30 (2014) 77–96. doi:10.1016/j.dental.2013.07.013.

[5] R.B. Cartwright, Dentinal hypersensitivity: a narrative review, Community Dent. Health. 31 (2014) 15–20.

[6] T. Saito, H. Toyooka, S. Ito, M.A. Crenshaw, In vitro study of remineralization of dentin: effects of ions on mineral induction by decalcified dentin matrix, Caries Res. 37 (2003) 445–449. doi:10.1159/000073398.

[7] J. Zhu, R. Liang, C. Sun, L. Xie, J. Wang, D. Leng, D. Wu, W. Liu, Effects of nanosilver and nanozinc incorporated mesoporous calcium-silicate nanoparticles on the mechanical properties of dentin, PloS One. 12 (2017) e0182583. doi:10.1371/journal.pone.0182583.

[8] M.G. Gandolfi, G. Ciapetti, P. Taddei, F. Perut, A. Tinti, M.V. Cardoso, B. Van Meerbeek, C. Prati, Apatite formation on bioactive calcium-silicate cements for dentistry affects surface topography and human marrow stromal cells proliferation, Dent. Mater. 26 (2010) 974–992. doi:10.1016/j.dental.2010.06.002.

[9] L. Xiao, D. Wu, X. Wang, W. Du, J. Zhang, S. Li, H. Zhou, J. Wu, Y. Tian, Four Novel Zn (II) Coordination Polymers Based on 4'-Ferrocenyl-3,2':6',3''-Terpyridine: Engineering a Switch from 1D Helical Polymer Chain to 2D Network by Coordination Anion Modulation, Mater. Basel Switz. 10 (2017). doi:10.3390/ma10121360.

[10] A.C. Ionescu, E. Brambilla, A. Travan, E. Marsich, I. Donati, P. Gobbi, G. Turco, R. Di Lenarda, M. Cadenaro, S. Paoletti, L. Breschi, Silver-polysaccharide antimicrobial nanocomposite coating for methacrylic surfaces reduces Streptococcus mutans biofilm formation in vitro, J. Dent. 43 (2015) 1483–1490. doi:10.1016/j.jdent.2015.10.006.

[11] M.A. Melo, S. Orrego, M.D. Weir, H.H.K. Xu, D.D. Arola, Designing Multiagent Dental Materials for Enhanced Resistance to Biofilm Damage at the Bonded Interface, ACS Appl. Mater. Interfaces. 8 (2016) 11779–11787. doi:10.1021/acsami.6b01923.

[12] K. Zhang, L. Cheng, S. Imazato, J.M. Antonucci, N.J. Lin, S. Lin-Gibson, Y. Bai, H.H.K. Xu, Effects of dual antibacterial agents MDPB and nano-silver in primer on microcosm biofilm, cytotoxicity and dentin bond properties, J. Dent. 41 (2013) 464–474. doi:10.1016/j.jdent.2013.02.001.

[13] R. Osorio, C.A. Alfonso-Rodríguez, A.L. Medina-Castillo, M. Alaminos, M. Toledano, Bioactive Polymeric Nanoparticles for Periodontal Therapy, PloS One. 11 (2016) e0166217. doi:10.1371/journal.pone.0166217.

[14] M. Toledano-Osorio, E. Osorio, F.S. Aguilera, A. Luis Medina-Castillo, M. Toledano, R. Osorio, Improved reactive nanoparticles to treat dentin hypersensitivity, Acta Biomater. 72 (2018) 371–380. doi:10.1016/j.actbio.2018.03.033.
[15] M. Toledano, M. Toledano-Osorio, A.L. Medina-Castillo, M.T. López-López, F.S. Aguilera, R. Osorio, Ion-modified nanoparticles induce different apatite formation in cervical dentine, Int. Endod. J. (2018). doi:10.1111/iej.12918.
[16] K.H.L. Kwan, X. Liu, M.K.T. To, K.W.K. Yeung, C. Ho, K.K.Y. Wong, Modulation of collagen alignment by silver nanoparticles results in better mechanical properties in wound healing, Nanomedicine Nanotechnol. Biol. Med. 7 (2011) 497–504. doi:10.1016/j.nano.2011.01.003.
[17] H. Geng, G. Poologasundarampillai, N. Todd, A. Devlin-Mullin, K.L. Moore, Z. Golrokhi, J.B. Gilchrist, E. Jones, R.J. Potter, C. Sutcliffe, M. O'Brien, D.W.L. Hukins, S. Cartmell, C.A. Mitchell, P.D. Lee, Biotransformation of Silver Released from Nanoparticle Coated Titanium Implants Revealed in Regenerating Bone, ACS Appl. Mater. Interfaces. 9 (2017) 21169–21180. doi:10.1021/acsami.7b05150.
[18] Y. Zhang, D. Zhai, M. Xu, Q. Yao, H. Zhu, J. Chang, C. Wu, 3D-printed bioceramic scaffolds with antibacterial and osteogenic activity, Biofabrication. 9 (2017) 025037. doi:10.1088/1758-5090/aa6ed6.
[19] Q.H. Zhi, E.C.M. Lo, A.C.Y. Kwok, An in vitro study of silver and fluoride ions on remineralization of demineralized enamel and dentine, Aust. Dent. J. 58 (2013) 50–56. doi:10.1111/adj.12033.
[20] A.L. Medina-Castillo, J.F. Fernandez-Sanchez, A. Segura-Carretero, A. Fernandez-Gutierrez, Micrometer and Submicrometer Particles Prepared by Precipitation Polymerization: Thermodynamic Model and Experimental Evidence of the Relation between Flory's Parameter and Particle Size, Macromolecules. 43 (2010) 5804–5813. doi:10.1021/ma100841c.
[21] S. Habelitz, M. Balooch, S.J. Marshall, G. Balooch, G.W. Marshall, In situ atomic force microscopy of partially demineralized human dentin collagen fibrils, J. Struct. Biol. 138 (2002) 227–236.
[22] W.C. Oliver, G.M. Pharr, An improved technique for determining hardness and elastic modulus using load and displacement sensing indentation experiments, J. Mater. Res. 7 (1992) 1564–1583. doi:10.1557/JMR.1992.1564.
[23] M. Toledano, R. Osorio, E. Osorio, A.L. Medina-Castillo, M. Toledano-Osorio, F.S. Aguilera, Ions-modified nanoparticles affect functional remineralization and energy dissipation through the resin-dentin interface, J. Mech. Behav. Biomed. Mater. 68 (2017) 62–79. doi:10.1016/j.jmbbm.2017.01.026.
[24] M. Toledano, R. Osorio, E. Osorio, F. García-Godoy, M. Toledano-Osorio, F.S. Aguilera, Advanced zinc-doped adhesives for high performance at the resin-carious dentin interface, J. Mech. Behav. Biomed. Mater. 62 (2016) 247–267. doi:10.1016/j.jmbbm.2016.05.013.
[25] M.D. McKee, Y. Nakano, D.L. Masica, J.J. Gray, I. Lemire, R. Heft, M.P. Whyte, P. Crine, J.L. Millán, Enzyme Replacement Therapy Prevents Dental Defects in a Model of Hypophosphatasia, J. Dent. Res. 90 (2011) 470–476. doi:10.1177/0022034510393517.
[26] M. Balooch, S. Habelitz, J.H. Kinney, S.J. Marshall, G.W. Marshall, Mechanical properties of mineralized collagen fibrils as influenced by demineralization, J. Struct. Biol. 162 (2008) 404–410. doi:10.1016/j.jsb.2008.02.010.

[27] L.E. Bertassoni, S. Habelitz, J.H. Kinney, S.J. Marshall, G.W. Marshall, Biomechanical perspective on the remineralization of dentin, Caries Res. 43 (2009) 70–77. doi:10.1159/000201593.
[28] A.G. Schwartz, J.D. Pasteris, G.M. Genin, T.L. Daulton, S. Thomopoulos, Mineral distributions at the developing tendon enthesis, PloS One. 7 (2012) e48630. doi:10.1371/journal.pone.0048630.
[29] R. Osorio, E. Osorio, I. Cabello, M. Toledano, Zinc induces apatite and scholzite formation during dentin remineralization, Caries Res. 48 (2014) 276–290. doi:10.1159/000356873.
[30] J.A. Timlin, A. Carden, M.D. Morris, R.M. Rajachar, D.H. Kohn, Raman Spectroscopic Imaging Markers for Fatigue-Related Microdamage in Bovine Bone, Anal. Chem. 72 (2000) 2229–2236. doi:10.1021/ac9913560.
[31] A. Kunstar, J. Leijten, S. van Leuveren, J. Hilderink, C. Otto, C.A. van Blitterswijk, M. Karperien, A.A. van Apeldoorn, Recognizing different tissues in human fetal femur cartilage by label-free Raman microspectroscopy, J. Biomed. Opt. 17 (2012) 116012. doi:10.1117/1.JBO.17.11.116012.
[32] L.K. Bakland, J.O. Andreasen, Will mineral trioxide aggregate replace calcium hydroxide in treating pulpal and periodontal healing complications subsequent to dental trauma? A review, Dent. Traumatol. 28 (2012) 25–32. doi:10.1111/j.1600-9657.2011.01049.x.
[33] H. Salehi, E. Terrer, I. Panayotov, B. Levallois, B. Jacquot, H. Tassery, F. Cuisinier, Functional mapping of human sound and carious enamel and dentin with Raman spectroscopy, J. Biophotonics. 6 (2013) 765–774. doi:10.1002/jbio.201200095.
[34] M. Toledano, F.S. Aguilera, E. Osorio, I. Cabello, M. Toledano-Osorio, R. Osorio, Functional and molecular structural analysis of dentine interfaces promoted by a Zn-doped self-etching adhesive and an in vitro load cycling model, J. Mech. Behav. Biomed. Mater. 50 (2015) 131–149. doi:10.1016/j.jmbbm.2015.05.026.
[35] L.C. Gruen, Interaction of amino acids with silver(I) ions, Biochim. Biophys. Acta. 386 (1975) 270–274.
[36] M.E. Matthiessen, B. Sögaard-Pedersen, P. Römert, Electron microscopic demonstration of non-mineralized and hypomineralized areas in dentin and cementum by silver methenamine staining of collagen, Scand. J. Dent. Res. 93 (1985) 385–395.

Table 1. Mean and standard deviation of nanohardness (*Hi*) (GPa) and Young´s Modulus (*Ei*) (GPa) values at dentin surfaces of the different experimental groups.

		Untreated		NPs		Ag-NPs	
		24h	7d	24h	7d	24h	7d
***Hi* (GPa) Mean (SD)**	ID	0.90 (0.22) A	0.85 (0.08) a	0.73 (0.16) A	0.88 (0.11) a	0.36 (0.11) B	0.42 (0.05) b
	PD	1.06 (0.06) A*	0.61 (0.06) a	0.77 (0.26) AB	0.68 (0.14) a	0.34 (0.17) B	0.45 (0.05) b
***Ei* (GPa) Mean (SD)**	ID	24.69 (1.52) A*	15.13 (0.90) a	23.60 (1.90) A	23.99 (1.85) b	9.05 (1.19) B	10.95 (1.25) c
	PD	25.94 (2.09) A*	19.28 (3.22) a	22.69 (2.49) A	20.06 (1.78) a	8.87 (3.53) B	12.89 (1.64) b

Same letter (capital for 24 h and lowercase for 7 d) indicates no significant differences between treatment groups at the same dentin type [intertubular dentin (ID) or peritubular dentin (PD)]. * indicates significant differences between the two storage periods (24 hours or 7 days) in the same treatment group and dentin type (ID or PD). Abbreviations: Ag-NPs: Ag doped nanoparticles; NPs: undoped nanoparticles; PD: peritubular dentin; ID: intertubular dentin.

Table 2. Raman intensities (in arbitrary units) of mineral and organic components in treated cervical dentin surfaces.

			Untreated		Undoped-NPs		Ag-NPs	
			24h	7d	24h	7d	24h	7d
Relative Presence of Mineral	Phosphate [961]	Peak	371.58	420.34	595.85	637.39	521.74	593.35
		Area	9400.72	10656.50	15054.00	16435.05	13496.60	15460.20
		RMC_P	25.07	33.15	25.42	24.87	22.91	20.99
	Carbonate [1070]	Peak	52.43	54.07	77.95	80.04	69.35	70.63
		Area	2052.87	2096.28	2849.10	2682.48	2820.31	2526.32
		RMC_C	3.54	4.26	3.33	3.12	3.05	2.50
Crystallinity	FWHM		19.31	19.36	19.29	19.35	19.75	19.89
***v2*[430]**			70.70	68.81	78.03	93.67	83.29	108.52
***v1*[954]**			309.61	318.07	502.85	541.61	403.94	519.52
***v1*[963]**			342.53	371.09	534.17	566.23	466.44	523.88
Normalization	Phenyl [1003]		14.82	12.68	23.44	25.63	22.77	28.27
Crosslinking	Pyridinium [1032]		23.03	19.78	27.98	28.58	39.62	38.42
Nature and secondary structure of collagen	CH_2 [1450]		25.13	19.11	27.23	27.00	45.26	27.64
	A-I [1655-1667]		7.57	4.07	4.65	4.43	5.24	5.27
	Ratio A-I/A-III		0.20	0.12	0.11	0.10	0.12	0.13

RMC_P: Relative Mineral Concentration between Phosphate/Phenyl (1003 cm^{-1}); RMC_C: Relative Mineral Concentration between Carbonate/Phenyl (1003 cm^{-1}); FWHM: Full-width half-maximum of the phosphate band at 961 cm^{-1}; A: amide.
Peaks positions are expressed in cm^{-1}. For the mineral components, the peaks values have been normalized to the basis intensity of the symmetric phosphate band, near 960 cm^{-1}. For the organic components, the peaks values have been normalized to the basis intensity of the Amide II band near 1510 cm^{-1}.

Figure 1

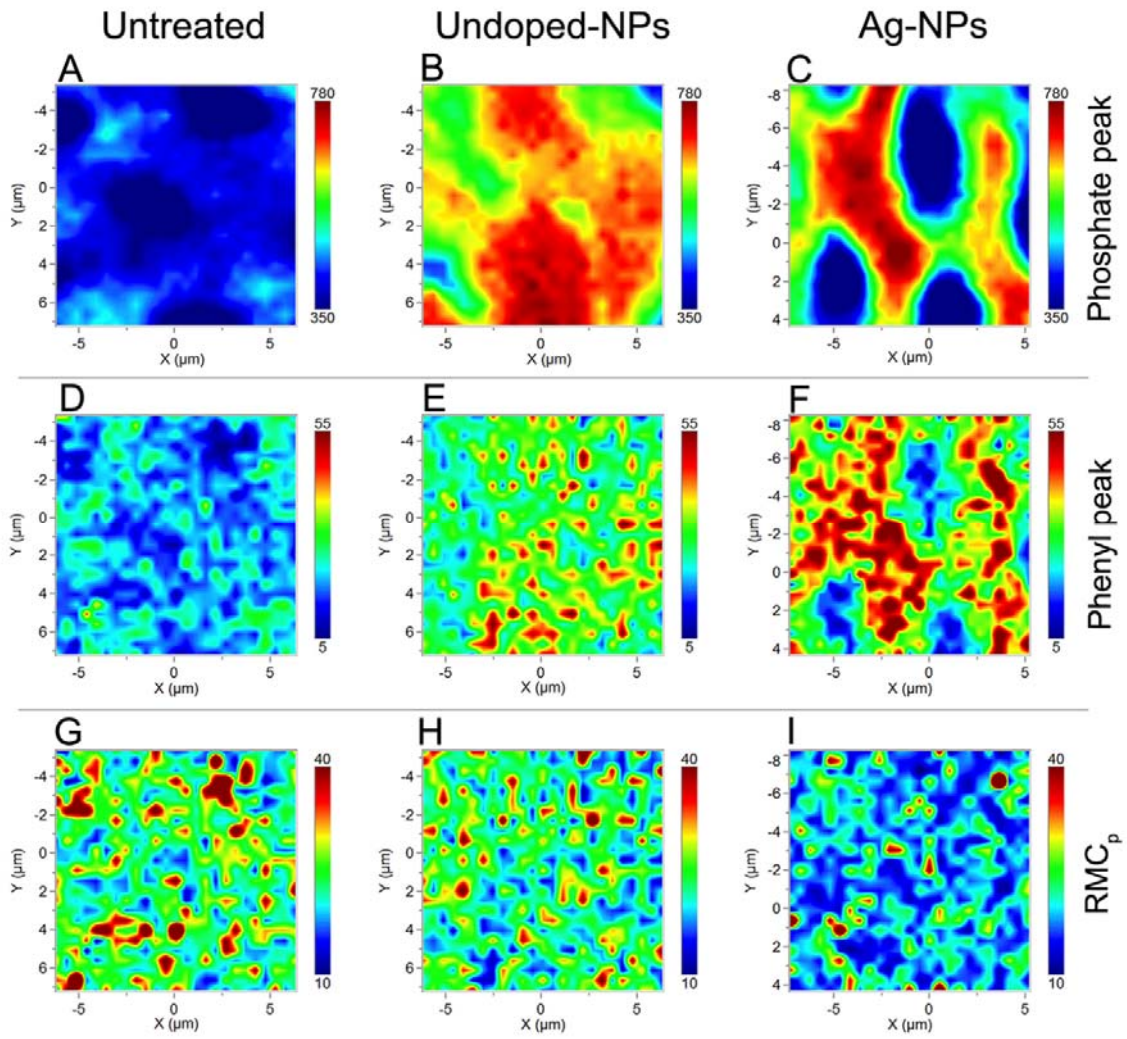

Figure 1. 2D micro-Raman map of the phosphate peak (961 cm^{-1}) intensities at untreated dentin (**A**), dentin treated with undoped-NPs (**B**), and dentin treated with Ag-NPs (**C**), after 7 d storage. 2D micro-Raman map of the phenyl group (1003 cm^{-1}) intensities at untreated dentin (**D**), dentin treated with undoped-Nps (**E**), and dentin treated with Ag-NPs (**F**), after 7 d storage. 2D micro-Raman map of the RMC_P [Relative mineral concentration between phosphate/phenyl (1003 cm^{-1})], at untreated dentin (**G**), dentin treated with undoped-NPs (**H**), and dentin treated with Ag-NPs (**I**), after 7 d storage. In the color scheme shown, the red color corresponds to high values of phosphate peak (**A to F**), or high values of RMC_P (**G to I**).

Figure 2

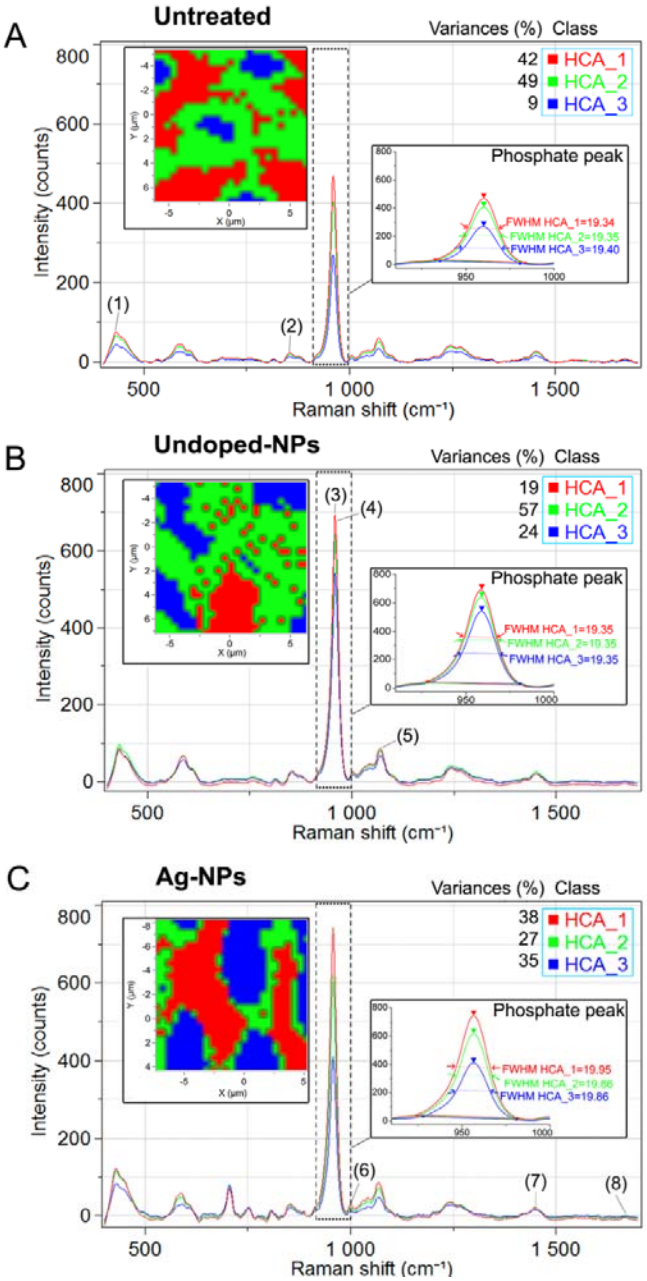

Figure 2. Raman spectra from hierarchical cluster analysis (HCA) results of untreated dentin (**A**), dentin treated with undoped-NPs (**B**), and dentin treated with Ag-NPs (**C**), after 7 d storage. The peaks position are marked with the numbers in parenthesis: (1) *v2* (430 cm^{-1}); (2) *v1* (954 cm^{-1}); (3) phosphate (961 cm^{-1}); (4) *v1* (963 cm^{-1}); (5) carbonate (1070 cm^{-1}); (6) pyridinium (1032 cm^{-1}); (7) CH_2 (1450 cm^{-1}); (8) Amide I (1655-1667 cm^{-1}). Top left insets are showing the color mapping from hierarchical cluster analysis (HCA) images. Three levels of HCA clustering are shown. Areas of distinct colors have differences in Raman spectral distribution and chemical composition. Each cluster is assigned to a different color (red, green and blue). Right insets are showing full width half maximum (FWHM) of the phosphate peak (961 cm^{-1}) at single truncated spectra points.

Figure 3

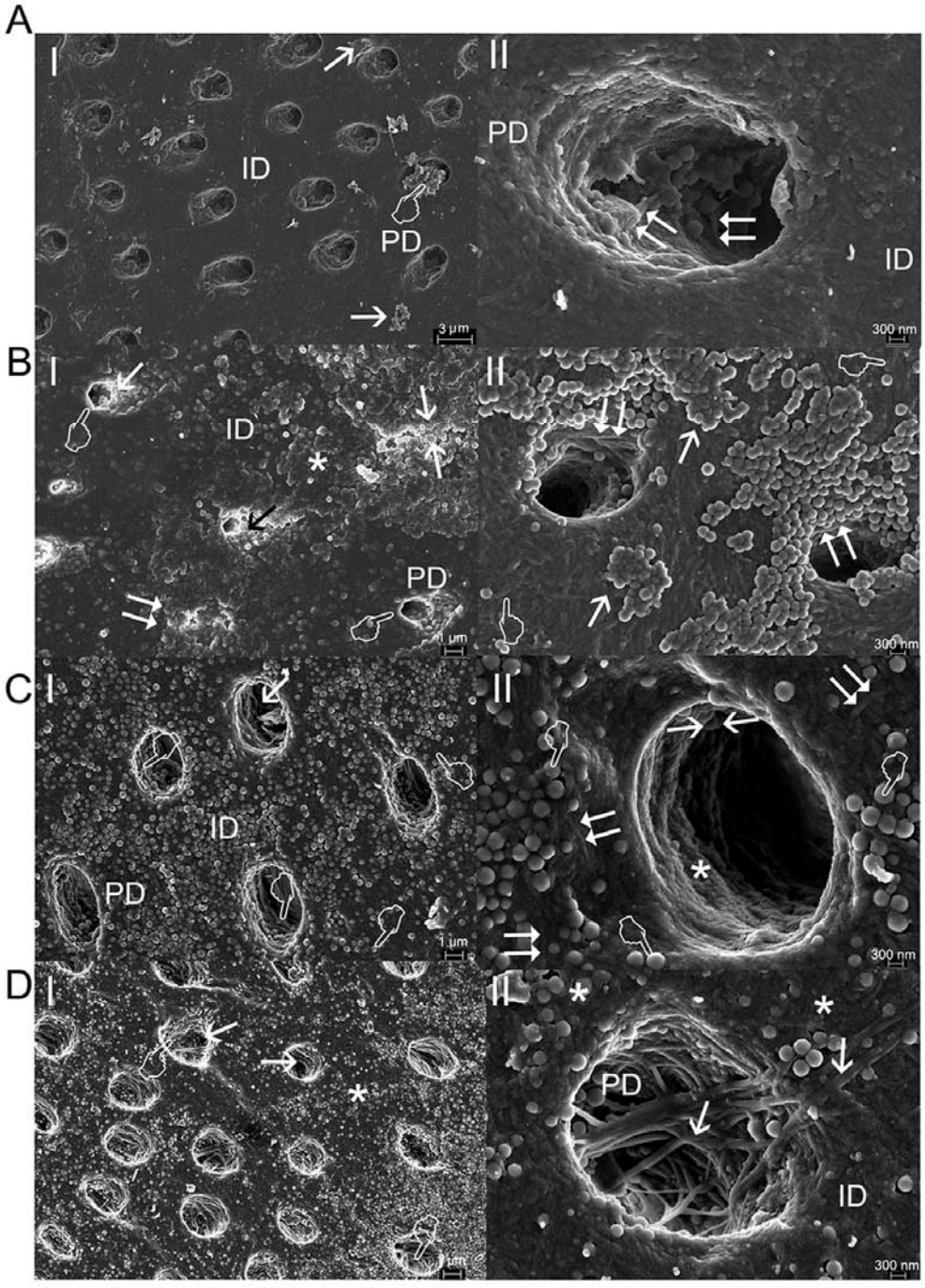

Figure 3. (**A**), Field emission scanning electron microscopy images of untreated dentin, after 24 h (**I**) and 7 d (**II**) of storage. A few crystals or mineral deposits were occasionally encountered at both intertubular and peritubular dentin (arrows). Some mineral deposits were observed at the tubule lumen (pointer). Tubules appeared mineral free with a clear ring of peritubular dentin (PD). Fully extrafibrillar mineralized dentin collagen is shown (double arrows). (**B**), Dentin treated with NPs after 7 d of storage. Peritubular (PD) and intertubular

dentin (ID) were strongly mineralized (**I**). A consistent and continuous layer of mineral is observed covering the intertubular dentin (asterisk). A robust PD was observed (pointers). Dentinal tubules appeared partially filled with mineral precipitates and mineralized NPs (arrows). Filled (double arrows) or covered (faced arrows) dentinal tubules were also evidenced. At high magnification (**II**), a layer of precipitated crystals appeared covering the intertubular and peritubular dentin. Some clustered and mineralized NPs appeared heterogeneously distributed at the dentin surface (arrows). A dense network of partially mineralized collagen fibrils, were observed covering the peritubular dentin (double arrows). The prototypical D-periodicity banding of collagen fibrils was scarcely noted (pointers). (**C**), Dentin treated with Ag-NPs after 24 h (**I**) of storage. A dense net of precipitated Ag-NPs covered both the intertubular (ID) and peritubular (PD) dentin. The tubule entrances appeared visible (arrow). Ag-NPs also penetrated the dentinal tubules and remained adhered to the tubule wall. Some intertubular and peritubular collagen fibrils were observed (pointers). At high magnification (**II**), a reticular pattern of staggered and demineralized collagen fibrils (doubled arrows) was observed covering the intertubular dentin. Mineralized dentin was also observed at intertubular and peritubular dentin areas (asterisks). Multiple and remineralized Ag-NPs (pointers) were homogeneously distributed throughout the ID, and some of them were observed within the lumen of the dentinal tubules (faced arrows). (**D**), Dentin treated with Ag-NPs after 7 d (**I**) of storage. An extended layer of minerals and collagen fibrils, that incorporated the Ag-NPs, occupied the intertubular dentin (asterisks). The tubule entrances appeared open (arrows). Some NPs infiltrated the lumen of the dentinal tubules (pointers). At high magnification (**II**), multiple Ag-NPs onto the dentin surface are shown (asterisks). Staggered and demineralized collagen fibrils (arrows) were observed covering both the intertubular (ID) and peritubular dentin (PD).